Journal Pre-proof

An exploration of equivalent scenarios for building facade fire standard tests

Yizhou Li, Zilong Wang, Xinyan Huang

PII: S2352-7102(22)00412-0

DOI: https://doi.org/10.1016/j.jobe.2022.104399

Reference: JOBE 104399

To appear in: *Journal of Building Engineering*

Received Date: 28 December 2021

Revised Date: 16 March 2022

Accepted Date: 19 March 2022

Please cite this article as: Y. Li, Z. Wang, X. Huang, An exploration of equivalent scenarios for building facade fire standard tests, *Journal of Building Engineering* (2022), doi: https://doi.org/10.1016/j.jobe.2022.104399.

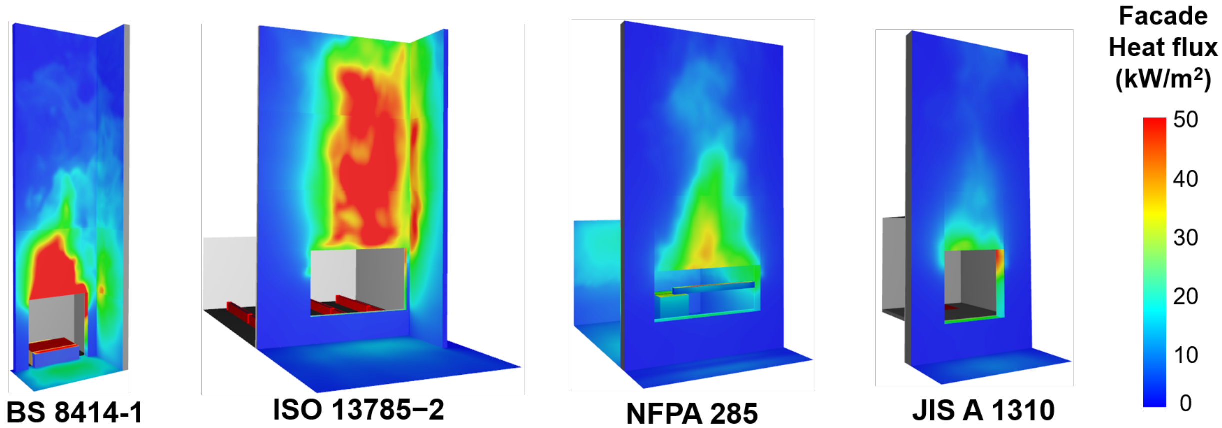
Facade
Heat flux
(kW/m²)
50
40
30
20
10
0
BS 8414-1
ISO 13785–2
NFPA 285
JIS A 1310

An Exploration of Equivalent Scenarios for Building Facade Fire Standard Tests

Yizhou Li[#], Zilong Wang[#], Xinyan Huang*

Research Centre for Fire Safety Engineering, Department of Building Environment and Energy Engineering, The Hong Kong Polytechnic University, Hong Kong

[#]These authors contributed to the work equally and should be regarded as co-first authors

*Corresponding to xy.huang@polyu.edu.hk (X. Huang)

Abstract: The building facade system is a key part of green buildings and carbon neutrality, but its fire safety is a global problem. Many large-scale facade fire standard tests are created to evaluate the fire risk of facade systems, but they are different from country to country, and their test results are difficult to compare. This study simulates five scenario-based facade fire standard tests, BS 8414-1 (UK), GB/T 29416 (China), ISO 13785-2, NFPA 285 (USA), and JIS A 1310 (Japan). Simulations explore the heat flux and temperature of spilled facade fire plume that controls the ignition and flame spread of facade fire. Under the default fire scenario, the BS 8414-1 and GB/T 29416 generate the largest heat flux (~100 kW/m^2) to ignite the facade above the opening. The facade fire plume in ISO 13785-2 produces a near-constant heat flux (~50 kW/m^2) for 2 m above the opening. The heat flux and plume temperature of NFPA 285 largely depend on the extra window burner, and JIS A 1310 can produce intensive heating on the facade by increasing the chamber fire heat release rate (HRR). The heat flux and temperature of spilled plume increase almost linearly with the outdoor fire HRR. Thus, by adjusting the total fire HRR, the values of surface heat flux, plume temperature, and ignition height can be matched to enable a fair comparison among different tests. This unique numerical work explores the equivalent façade fire scenarios for different standard tests that can guide future façade fire test development and optimization.

Keywords: *Fire simulation; Spilled flame; Facade fire tests; Heat release rate; Heat flux;*

1. Introduction

The building facade system is developed for beauty and energy-saving, and it is a key part of green buildings and carbon neutrality [1–3]. However, the existence of facade systems paves the way for the propagation of facade fire [4] if the facade system includes combustible and flammable materials [5,6]. So far, many facade fire accidents have happened globally because of unsafe and non-fireproof facade systems, resulting in hundreds of deaths and huge economic losses. The famous fire accidents include the 2010 Shanghai Jing'an fire with 58 victims (Fig. 1a), the 2015 Dubai Address Tower fire (Fig. 1b), and the 2017 London Grenfell Tower fire with 72 victims [7,8] (Fig. 1c). These tragedies show the importance of understanding the fire risk of the building facade.

For a long time, the manner in evaluating the performance of facade systems was to rate the combustibility levels of the individual material [6]. However, these kinds of material fire tests are recognized as not suitable for assessing the facade component, facade systems, or their reaction to fire. Gradually, more facade fire standard tests are proposed to evaluate the fire risk in the component and system levels, such as the scenario tests and corner tests [6,9]. Relatively, scenario tests are regulated more widely than corner tests. The term "scenario tests" refers to setting up a compartment fire scenario and creating the spilled flame and plume on the facade to simulate the ignition of facade materials and the vertical flame spread on the facade. The scenario-based facade fire tests are large-scale that can simulate the reaction-to-fire and then be adopted in many countries [10–14].

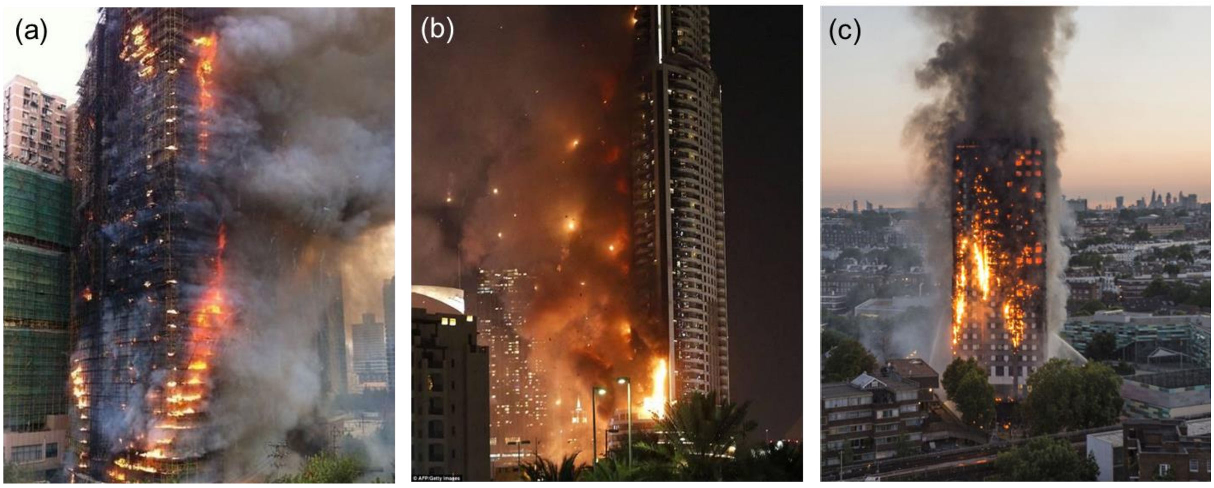

Fig. 1. (a) Shanghai Jing'an fire in 2010, (b) Dubai Address Tower fire in 2015, (c) London Grenfell Tower fire in 2017.

However, the large-scale facade fire test setups, procedures, and acceptance criteria vary from country to country [15]. Can we fairly compare the results from different standards tests? Will the tests of the same facade sample get significantly different results and ratings under different standard fire tests? For example, if the sample passes the test of NFPA 285 in the USA, can it meet the requirements of BS 8414-1 in the UK[10]? These differences in tests and acceptance criteria not only create many misunderstandings and disputes but also prevent data sharing and comparison, eventually hindering the global facade fire safety. Thus, it is necessary to provide a scientific guideline to compare different facade fire standard test and summarize their equivalent testing conditions.

Many researchers performed experiments and numerical simulations to test the facade sample performance based on a single standard test, which aimed to determine if it meets the fire resistance regulations [16–23]. For example, Zhou *et al.* [16,17] conducted a group of tests to judge the thermoplastic expanded polystyrene's (EPS) facade combustibility according to the JIS A 1310. Agarwal *et al.* [18] tested cladding assemblies according to ANSI/FM 4880 to evaluate their combustibility. Jansson and Anderson [19] evaluated the fire behaviors of the SP Brand 105 test method numerically and experimentally. Van Hees [20] studied the development process of the ISO facade fire standard test for the facade. Hostikka and Bytskov [21] used numerical methods to simulate the thermal environment on the facade in ISO 13785-2. Many other studies investigated the characteristics of spilled façade flame from the compartment, e.g., [24–26].

Although the behaviors of facade fire have been studied for many decades [27], few researchers have made a comparison of different facade fire standard tests. Anderson et al. [28,29] modeled the fire exposure and plume temperature in three standard facade fire tests, SP Brand 105, BS 8414-1, and the ISO 13785-2, and they called for the establishment of a unified facade fire standard test in Europe after comparing some European tests. One major problem is that although hundreds of large-scale facade fire tests were conducted for many different facade samples, most of these data and results are not disclosed by the manufacturers. Although some recognized laboratories were responsible for these standard tests, they often refused to make results public due to commercial reasons [30].

This study aims to simulate different facade fire tests and seek the equivalent façade fire. Numerical simulations are conducted to explore the spilled flame behaviors in five typical scenario-based facade fire tests. The spilled flame that acts as the ignition source of the facade sample and provides a hot environment for vertical flame spread is simulated and analyzed. Then, the equivalent fire HRR of each test that creates the same fire heating conditions on the facade sample is determined to form a common ground of comparison among different tests. The revealed equivalent fire scenarios will benefit the analysis of existing data, the mutual recognition of different tests, and the optimization of future facade fire standard tests. This work will provide a basis to link scenario-based facade fire standard tests and explore the equivalent façade fire scenarios for different tests.

2. Overview of facade fire standard tests

In general, the facade fire test scales can be divided into the micro scale (e.g., TG-DSC), small scale (e.g., cone calorimeter, ASTM E1321-97a LIFT, and UL94 tests), intermediate scale (e.g., ISO 13785-1), and the large scale (or full-scale). The cost of micro- and small-scale material tests is low, and several research groups have formed the fire test database for a large number of materials and facade samples [5,31,32]. As the test scale increases, the results are closer to real facade fires, but the cost of the test increases significantly, and the available number of large tests decreases (Fig. 2). Nevertheless, larger test sample and system are more complex (e.g., the combination of different materials and layers) that requires more tests to quantify and analyze the results. Therefore, more computational studies are needed to help analyze large-scale facade tests.

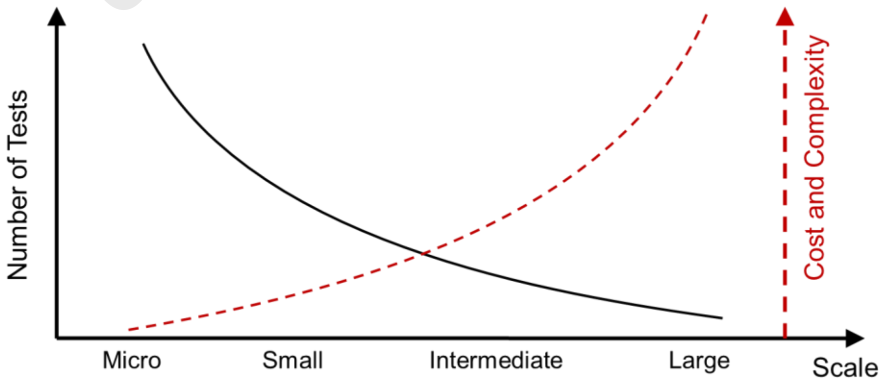

Fig. 2. Relationship between the number of tests, cost/complexity, and test scale.

This work numerically simulates five scenario-based facade fire standard tests, including BS 8414-1: 2020 (UK) [10], GB/T 29416: 2012 (China) [11], ISO13785-2: 2002 [12], NFPA 285: 2019 (USA)

[13], and JIS A 1310: 2019 (Japan) [14]. The ISO 13785-2 is a facade fire standard test regulated by ISO/TC 92/SC 1 (Fire initiation and growth), which is recognized by many countries. Note that this study neither recommends any specific standard test nor judges whether these tests are good or bad, strict or not. Instead, this paper aims to provide a new angle to understand these newest-version test methods so that they are kept updated to meet the fire safety requirements.

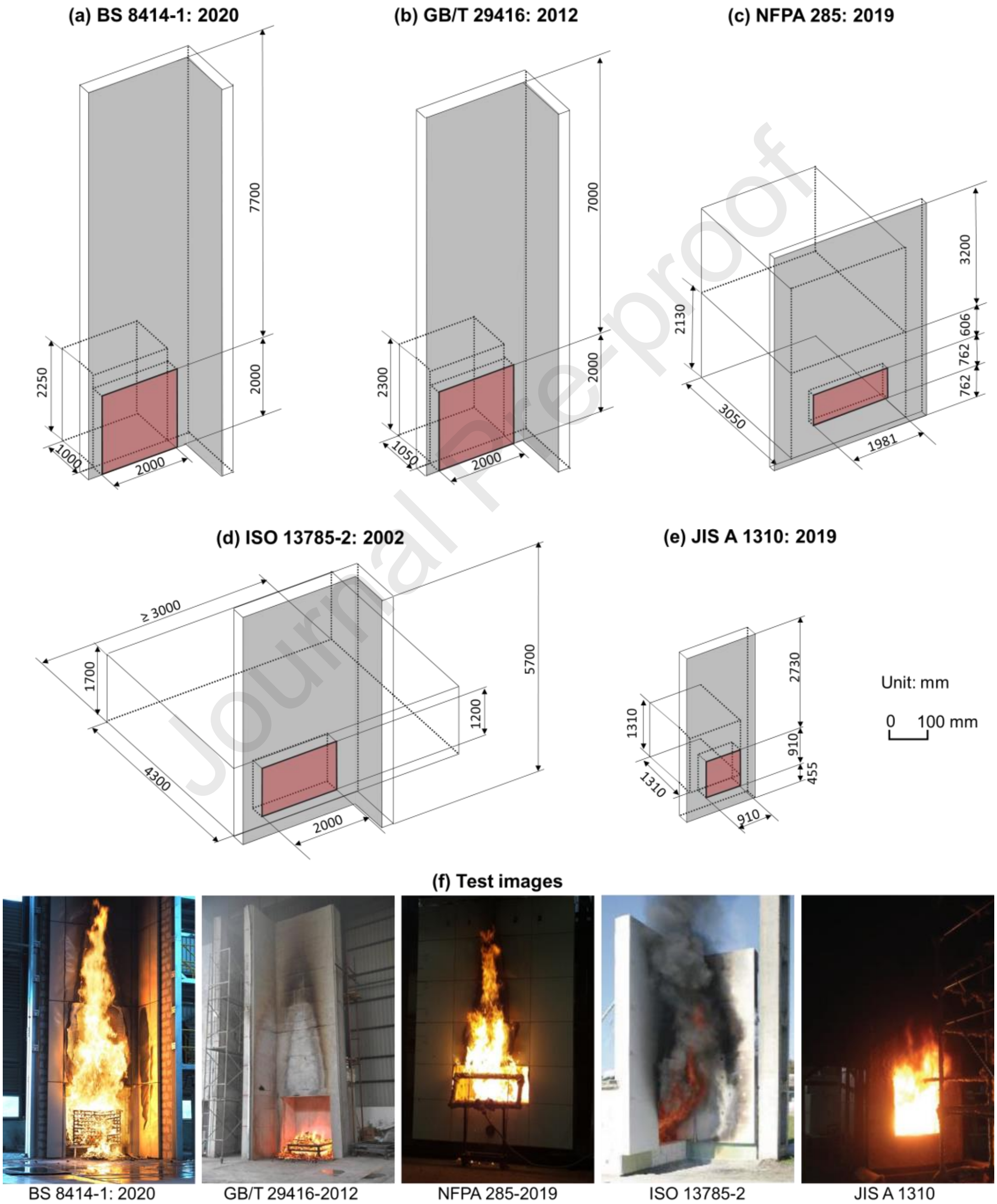

Fig.3. (a) GB/T 29416-2012 (China), (b) BS 8414-1: 2020 (UK), (c) ISO 13785-2, (d) NFPA 285-2019 (USA) and (e) JIS A 1310: 2019 (Japan), and (f) typical tests images [33].

All these test sets consist of combustion chambers and exterior walls, simulating the real compartment fire to assess the samples' fire-resistant performance. The detailed dimensions of five standard fire tests are shown in Fig. 3 and summarized in Table 1. The quantitative analysis and simple comparison are given below.

Table 1. Detailed comparisons of five facade fire standard tests.

Facade fire standard tests	**BS 8414-1: 2020 (UK)**	**GB/T 29416: 2012 (China)**	**NFPA 285: 2019 (USA)**	**ISO 13785-2: 2002**	**JIS A 1310: 2019 (Japan)**
Ignition source	Wood crib	Wood crib	Natural Gas	Propane	Propane
Set peak HRR [kW]	3,000	3,000	900 + 400	5,600	~900
Kawagoe HRR_{max}^* [kW]	8,485	8,485	1,976	3,944	1,185
Fire test time [min]	30	36	30	23-27	25
Chamber size* (L × W × H) [mm]	2,000 × 1,000 × 2,250	2,000× 1,050 × 2,300	3,050× 3,050 × 2,130	4,000× 4,300 × 1,700	1,350×1,350 × 1,350
Chamber volume, V (m^3)	4.50	4.83	19.8	43.9	2.46
Inner fire power density (kW m^3)	667	621	45.4	128	366
Opening size (W× H) [mm]	2,000 × 2,000	2,000 × 2,000	1,981 × 762	2,000 × 1,200	910 × 910
Front wall (L× H) [mm]	2,600 × 9,700	2,600 × 9,000	4,060×5,330	3,000 × 5,700	1,820 × 4,095
Side wall (L× H) [mm]	1,500 × 9,700	1,500 × 9,000	N/A	1,200 × 5,700	N/A
Total facade size (front + side) [m^2]	35.8	32.9	20.1	21.5	6.6
Front facade size (w/ opening) [m^2]	21.2	19.4	20.1	14.7	6.6
Peak surface heat flux (kW/m^2)	N/A	45-95	75	55±5 (within 0.6 m)	30±5 (within 0.9 m)

There are certain similarities and differences among these standard tests. The establishment of Chinese GB/T 29416 mainly refers to the BS 8414-1 (2002-year version), so it will not be discussed separately in this paper. The NFPA 285 and JIS A 1310 do not have sidewall facades. For the total facade sample size, it ranges from 6.62 m^2 to 35.77 m^2, while if only the front facade without the opening is considered, it ranges from 6.62 m^2 to 21.22 m^2. The fire chamber size ranges from 2.46 m^3 (JIS A 1310) to 43.86 m^3 (ISO 13785-2), where the JIS A 1310 has a cubic fire chamber. The opening of the fire chamber ranges from 0.83 m^3 (JIS A 1310) to 4.00 m^3 (BS 8414-1), where BS 8414-1, GB/T 29416, and JIS A 1310 have a square opening.

For the chamber fire source and scenario, the BS 8414-1 choose the wood crib while the other three tests choose the gas fuels of natural gas or propane. For an easy comparison, the maximum chamber fire heat release rate (HRR) calculated by Kawagoe (HRR = 1.5 W×$H^{1.5}$ [34]) is also listed to help assess the ventilation conditions of compartment fire and the intensity of the spilled flame, where only the ISO 13785-2 sets an HRR larger than the Kawagoe limit. The JIS A 1310-2019 recommended chamber fire HRR to be around 900 kW (increased from 600 kW in version 2015), so the actual tests can choose more severe fire scenarios. The NFPA 285 has an additional burner (400 kW) outside the combustion chamber to heat and ignite the facade sample, which is also different from all other tests. Their burning durations are also different, ranging from 23 to 36 minutes. These tests also require the heat flux on the surface of the facade sample to be either above a threshold value or in a recommended range, ensuring a sufficiently large chamber fire to heat the facade (Table 1).

In terms of the test scale, all five standard tests assess large-scale (or full-scale) facade samples. Therefore, these standard tests are generally considered large-scale facade fire tests, despite the different sizes of combustion chambers and openings. The JIS A 1310 has the smallest combustion chamber and opening among five tests, but the tested facade sample (6.62 m^2) is still much larger than the 4.32 m^2 of ISO 13785-1 intermediate corner test [35], and its opening height (910 mm) is higher than the opening height of NFPA 285 (762 mm).

3. Numerical methods

All the above facade fire standard tests are simulated numerically using FDS 6.7.5 [36], which uses the Large Eddy Simulation (LES) method to solve the conservation equations under fire scenarios. The effectiveness of FDS to simulate facade fire standard tests has been validated by many studies [21–24,28,29]. Past simulation results show good correspondence in terms of magnitude and distribution of experimental data. This work will focus on the use of numerical simulation in exploring the equivalent scenarios for different building facade fire standard tests.

In the numerical simulation, the HRRs of the ignition sources specified in the standard test are summarized in Fig. 4. These curves of HRRs are based on the given conditions in the standard test. NFPA 285 and ISO 13785-2 sets fuel flow rates, which can be calculated into HRRs. The HRR of JIS A 1310 is regulated and kept stable during the test. For the British standard, BS 8414-1 provided the detailed HRR progress in the test process, but the latest version of BS 8414-1 did not offer such a key parameter, so it is estimated according to the old version. Simultaneously, there is another difference that BS 8414-1 regulates that the crib is distinguished 30 min after ignition. Thus, the HRR of BS 8414-1 is calculated based on its version in 2002, but the fire test time is down to 30 min. However, GB/T 29416 used the same wood crib type as BS 8414-1 (2002) without fire suppression, so it can last for 36 min. These points are clearly shown in the below figure.

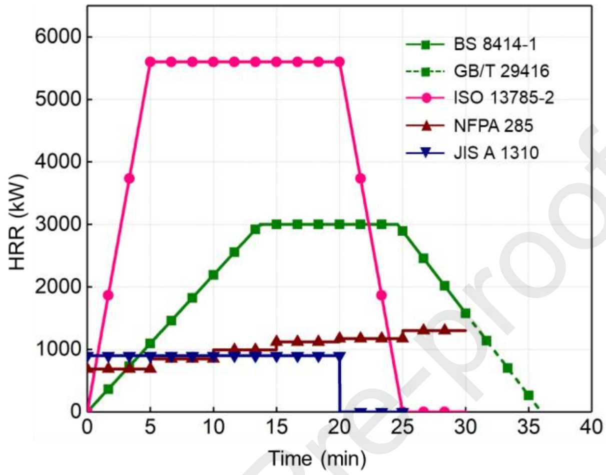

Fig. 4. HRRs of the ignition sources for each facade fire standard test.

Since the test scenario of Chinses Standard GB/T 29416 is very similar to BS 8414-1, their simulations results are essentially the same, so that only the simulation result of BS 8414-1 is presented to represent the GB/T 29416. As shown in Fig. 4, different HRRs are adopted in five facade fire standard tests. ISO 13785-2 has the largest peak HRR of the five standard tests (5,600 kW), while BS 8414-1 (GB/T 29416) has the second-highest peak HRR of 3,000 kW. The peak HRRs of NFPA 285 and JIS A 1310 are 1,300 kW and 900 kW, respectively. It should be noted that the NFPA 285 has a special burner at the opening of the combustion chamber to heat the test sample, and the JIS A 1310 specifies the recommended HRR of the ignition fire source (900 kW), which is maintained during the test.

The walls for each standard test are made of concrete with a density of 2,280 kg/m^3, a thermal conductivity of 1.8 W/m-K, and a specific heat capacity of 1.04 kJ/kg- K [37]. The effects of thermal conductivity of the walls as well as ventilation conditions are considered in the simulations. Parameters to be measured in each standard test include (1) the indoor and outdoor HRR during the test, (2) gas temperatures distribution at the central plane of the chamber and facade, and (3) gauge heat flux distribution on the facade. The mesh resolution of the simulation is determined using the dimensionless parameter D^*/δ_x, which should have a value not less than 10 to give satisfactory results [38], where D^* is the characteristic diameter of the fire source and δ_x is the nominal grid size.

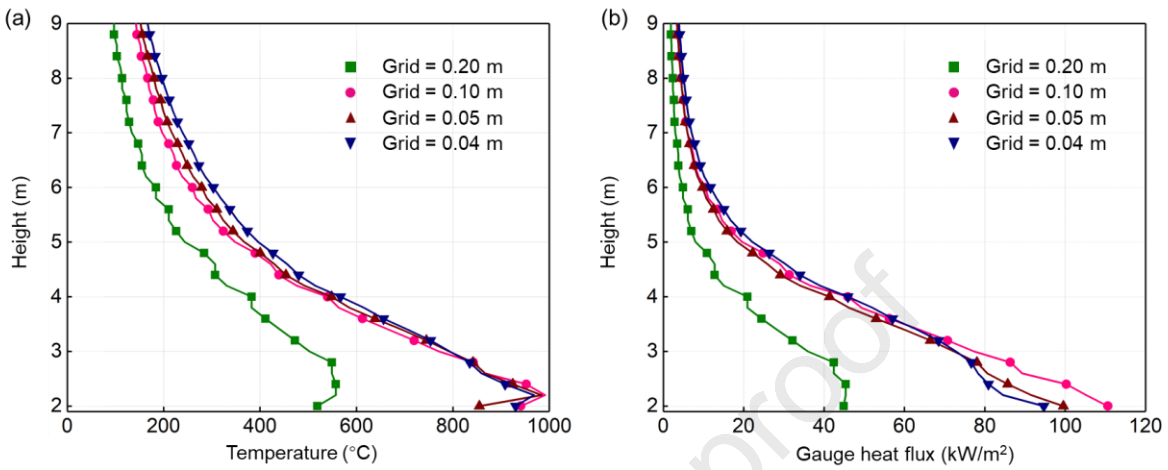

Fig. 5. Grid resolution effect on the distribution of (a) temperature and (b) gauge heat flux at the centerline of the facade in BS 8414-1.

According to the HRR given by each test, the final grid size of 0.05 m was selected for all the facade fire standard tests. This size is same or finer than the grid size adopted by other researchers [21,22,39,40] to give more accurate results. To further verify the quality of the grid size, a grid sensitivity study was conducted by simulating the test scenario of BS 8414-1. Four different mesh resolutions were considered: (1) 0.20 m, (2) 0.10 m, (3) 0.05 m, and (4) 0.04 m. The average gas temperature and gauge heat flux from 900 s to 1,400 s at the centerline of the facade sample are shown in Fig. 5. Based on the grid sensitivity analysis, the temperature and gauge heat flux distribution at the centerline of the facade when using the grid of 0.05 m are close to the modeling results with a finer grid of 0.04 m. Similar results were found in other cases. Thus, the grid size of 0.05 m is sufficient to guarantee the grid independence of the computational results. A detailed validation by comparing simulation results with the test data also shows the accuracy of the model for façade fires, as shown in Fig. A1. Overall, our simulation results successfully reproduce the temperature profile and heat flux distribution of the large-scale facade test. All simulation results are within the acceptable ranges that are specified in the standard.

4. Numerical results

4.1. Fire heat release rate

The HRR is one of the most critical parameters in characterizing the fire behavior and thermal effects of the facade fire standard test. During the test, the indoor and outdoor HRRs are determined by the fire sizes of ignition sources and openings in the combustion chamber. The HRR development in each standard test is shown in Fig. 6. The HRRs in both over-ventilated stage and under-ventilated stage are measured and compared among these five standard tests. It is found that the maximum indoor HRR of ISO 13785-2 is the largest (~2,600 kW), much higher than BS 8414-1 (1,700 kW), NFPA 285 (750 kW), and JIS A 1310 (500 kW). After the total HRR reaches a critical value (under-ventilated stage), the indoor HRR gradually remains constant for all tests. The NFPA 285 sets an additional ignition fire source (gas burner) at the opening, so it will not affect the indoor HRR.

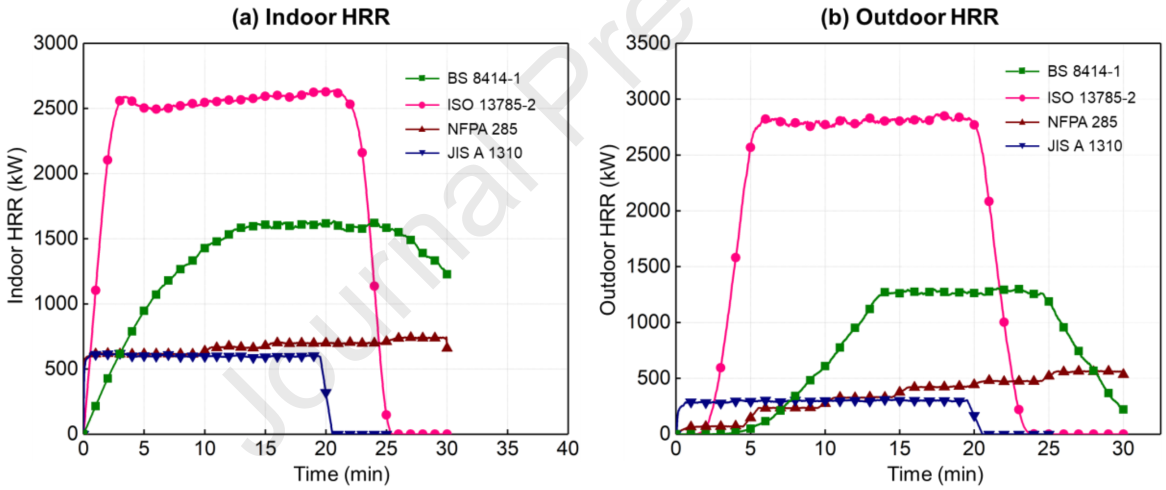

Fig. 6. (a) Indoor HRR and (b) Outdoor HRR for each facade fire standard test, the curve of BS 8414-1 is consistent with that of GB/T 29416

According to the Kawagoe equations, the indoor HRRs of these tests fail to reach the theoretical maximum HRRs except ISO 13785-2 (Table 1). It is because the sizes of actual burning areas are similar to the opening sizes, and the fuel supply rate is so high that the fuel does not mix well with the air inside the compartment, ultimately causing more fuel to be burned outside. This is a designed way to generate the spilled flame to test the samples.

The outdoor HRR for each standard test is also measured, which is the most direct parameter to reflect the intensity of spilled flames in the test. Fig. 6b shows that ISO 13785-2 has the highest outdoor HRR among five fire tests, the peak of which can reach around 2,800 kW. It is two times more than that of BS 8414-1, which is 1,400 kW in the outdoors, the second-highest among the five tests. For NFPA 285, the spilled flame is not only generated by the ignition source in the chamber but also from the burner placed near the top of the first-story window opening. Therefore, the HRR keeps increasing when more natural gas in the burner is provided. The maximum outdoor HRR of NFPA 285 is about 600 kW, still lower than that of BS 8414-1. Furthermore, JIS A 1310 has the lowest outdoor HRR, which is merely 300 kW. This value remains constant throughout the test process. What is noteworthy is that the HRR specified in the Japanese test is the recommended value, and a higher HRR is usually adopted in real tests. Therefore, it is necessary to pay attention to the actual HRR during the test when judging the JIS A 1310 test results.

4.2. Temperature of spilled fire plume

In addition to fire HRRs, the temperature profile of spilled fire plume on the facade surface is another criterion to describe the spilled façade flame behavior that can reflect the inner-building fire scenario [41]. The gas temperature distribution under the peak fire HRR for each standard test is compared in Fig. 7(a). The highest temperature area is distributed close to the opening upper, both inside and outside the chamber. Inside the combustion chamber, the temperature of BS 8414-1 test is the highest because it sets the largest fire power density (667 kW/m^3, see Table 1). Besides, its spilled fire-plume temperature is also clearly higher than all other three standard tests. The ISO 13785-2 test has a relatively high temperature inside the combustion chamber, considering its chamber is the largest. For NFPA 285, its peak temperature is outside the chamber due to the additional burner near the opening.

Fig. 7(b) further shows the simulated gas temperature distribution at the centerline of the facade above the opening. Based on the different spilled-flame phenomena, three regimes can be found with different plume temperatures,

(1) Continuous spilled flame (>560 ℃),

(2) Intermittent spilled flame (300 – 560 ℃), and

(3) No spilled flame (< 300 ℃).

In general, the pyrolysis temperature of polymers is above 300 ℃ [34], so the risk of ignition in the no-spilled-flame region is small. For the sample tests, the continuous-spilled-flame region should be mainly focused on as to the flame characteristics.

For the ISO 13785-2 test, the modelled gas temperature between 0.2 m and 1.2 m distant from the middle of the opening upper (~815 ℃) is almost stable, where the continuous flame covers most parts in the facade. The reason lies at its highest outdoor HRR, generating a large and continuous spilled flame near the opening. Although the BS 8414-1 test has the highest gas temperature at the opening upper, it decreases sharply when the gas is farther away from the opening. The highest temperature (~900 ℃) appears at the centerline where is 0.2 m high compared to the upper opening edge.

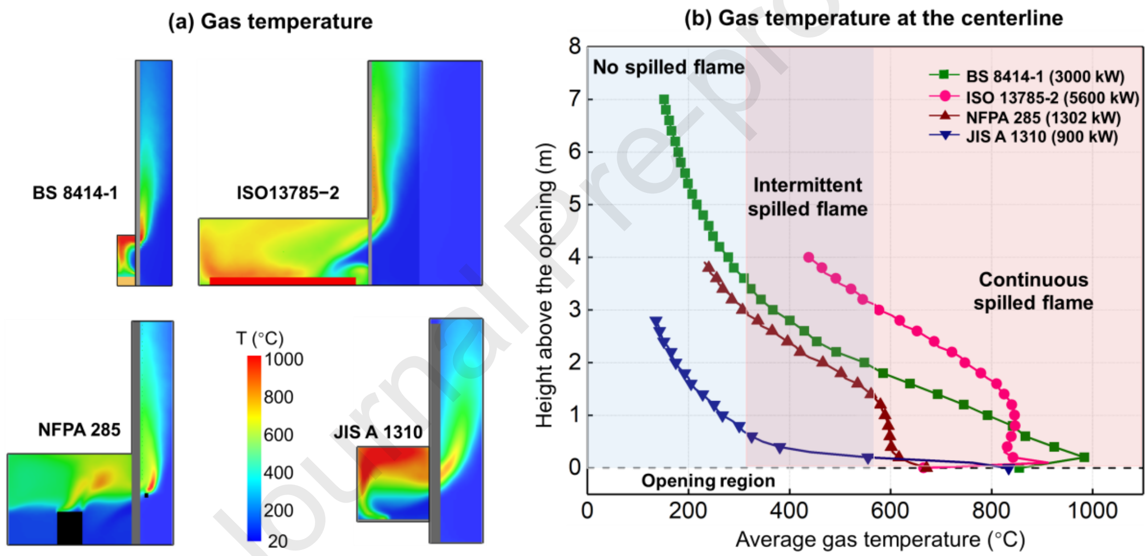

Fig. 7. (a) Gas temperature distribution of different facade tests at the peak fire HRR (not to scale), and (b) the average gas temperature at the centerline above the opening.

The NFPA 285 test has a stable gas temperature distribution (~600 ℃) in the area lower than 1.2 m height. Although it has a similar spilled flame behavior as BS 8414-1, its high-temperature plume is largely attributed to the extra window burner outside the chamber. The JIS A 1310 test has the smallest heating effect on the facade, considering the gas temperature distribution at the centerline of the facade is relatively lower than all other tests. Although the temperature can reach around 820 ℃ in the middle of the upper opening edge, it decreases sharply below 300 ℃, so there is only a small area of intermittent spilled flame. Nevertheless, if the fire HRR in JIS A 1310 is set higher, it can also generate a hotter spilled fire plume (discussed in Section 5).

Table 2 further summarizes the modeled peak temperature of the spilled fire plume, ranking as BS (984 ℃) > ISO (911 ℃) > JIS (834 ℃) > NFPA (671 ℃). The effective heating height on the facade above the opening can also be characterized by different threshold fire plume temperatures. For example, in the ISO test, the entire facade sample above the opening is above 400 ℃; and within 2.9 m above the opening, the plume temperature is above 600 ℃ (hot enough for auto-ignition), indicating the largest heating effect. Take the test conditions of more than 500 ℃ as an example (Table 2), and it is found that the effective ignition point height in four tests is around 2.2 m, 1.8 m, 3.6 m, and 0.3 m above the opening, respectively.

Table 2. Modeled flame and fire characteristics at the centerline of the facade for different tests.

Test parameters	**Threshold**	**BS 8414-1 or GB/T 29416**	**NFPA 285**	**ISO 13785-2**	**JIS A 1310**
Peak fire HRR [kW]	-	3,000	1,300	5,600	900
Peak outdoor HRR [kW]	-	1,400	600	2,800	300
Peak gas temperature on facade [℃]	-	984	671	911	834
Peak heat flux on facade [kW/m^2]	-	100	32	53	30
Effective ignition height (above opening) [m]	>300 ℃	3.6	3.0	>4	0.8
	>400 ℃	2.8	2.4	>4	0.4
	>500 ℃	2.2	1.8	3.6	0.3
	>600 ℃	1.7	1.0	2.9	0.2
Effective ignition height (above opening) [m]	>15 kW/m^2	3.3	1.6	>4	0.6
	>20 kW/m^2	2.9	1.0	3.9	0.3
	>30 kW/m^2	2.4	0.2	3.4	0
	>40 kW/m^2	2.0	0	2.8	0

4.3. Heat flux on facade surface

To further quantify the heating effect of the spilled fire plume on the facade sample, the heat flux on the facade surface at the peak fire HRR is shown in Fig. 8(a). Overall, the surface heat flux distribution is nearly symmetrical in all tests, with the peak value at the centerline of the opening. For the BS 8414-1 and ISO 13785-2 tests, the peak heat flux and the area of the high heat-flux region are clearly larger. The heat flux on their side facade wall is also high but still lower than the front facade.

For the NFPA 285 test, the modeled heat flux is relatively smaller because of a smaller fire HRR, and the surface heat flux mainly comes from the window burner. For JIS A 1310 test, it has the lowest heat flux on the facade due to the minimum fire HRR (900 kW) specified in the standard.

Fig. 8(b) further shows the surface heat flux at the centerline of the front facade. Similar to the temperature profile in Fig. 7(b), the heat flux profile can be divided into three regimes, (1) Continuous spilled flame (>36 kW/m^2), (2) Intermittent spilled flame (10 - 36 kW/m^2), and (3) No spilled flame (< 10 kW/m^2). For the BS 8414-1 test, it has a peak heat flux of about 100 kW/m^2 right above the opening because of the highest fire plume temperature; and then it becomes quickly below 10 kW/m^2, as the height is 4 m above the opening. For the ISO 13785-2 test, the highest outdoor HRR (2,800 kW/m^2 see Fig. 6(b) and Table 2) causes a strong spilled flame that covers a large facade surface. Thus, it causes a uniform high heat flux region (> 40 kW/m^2) for more than 3 m above the opening, although its peak heat flux is smaller than the BS 8414-1 test. In terms of surface heat flux profile, the NFPA 285 and JIS A 1310 tests are small and similar because of the low outdoor HRR.

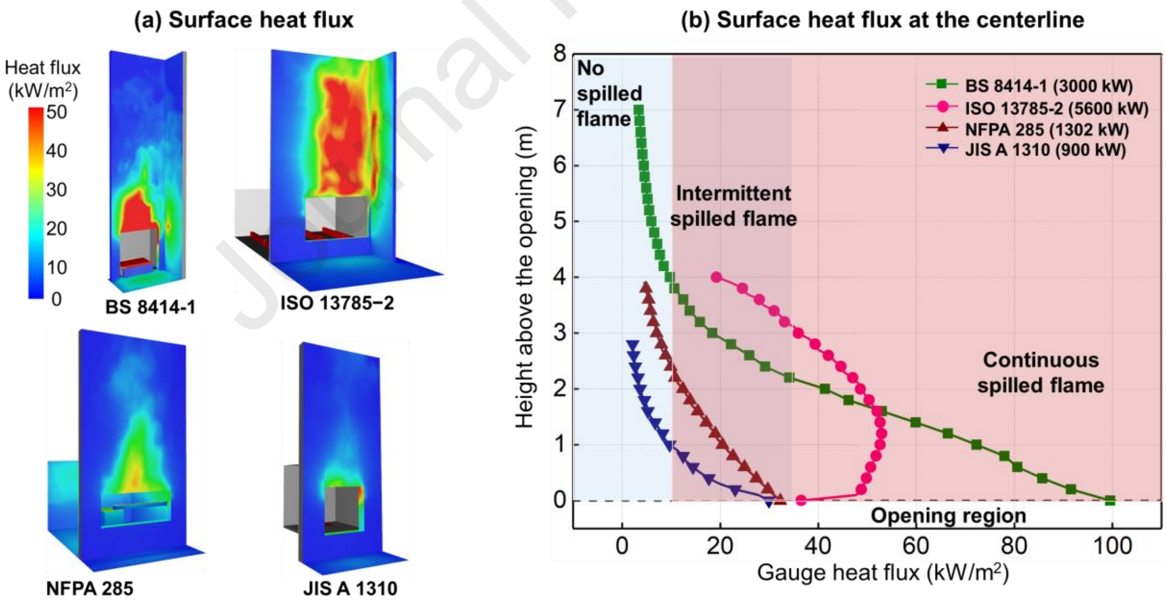

Fig. 8. (a) Surface heat flux distribution at the peak fire HRR (not to scale), and (b) the average heat flux of the facade surface at the centerline above the opening.

Besides, Table 2 further summarizes the modelled peak surface heat flux on the facade surface under the default test scenario, ranking as BS 8414-1 (100 kW/m^2) > ISO 13785-2 (53 kW/m^2) > NFPA 285 (32 kW/m^2) > JIS A 1310 (30 kW/m^2). The effective heating and ignition height on the facade above the opening can also be characterized by different threshold heat fluxes. For example, in the BS 8414-1 test, the 3.3 m above the opening is above 15 kW/m^2 (i.e., the minimum heat flux for piloted ignition). For the NFPA 285 test, the effective heating height above 15 kW/m^2 is about 1.6 m.

5. Equivalent fire scenarios

In the last section, the indoor and outdoor fire HRRs, spilled plume temperature, and heat flux on the facade sample have been determined under the default tests condition. Now, let us come back to our original questions, (1) how to fairly compare the fire performances of a facade sample under different standard tests, and (2) are there equivalent fire scenarios for different facade fire standard tests? To find out the equivalent fire scenarios (i.e., the fire HRR set inside the chamber) facade, time-dependent (transient) HRRs are set for the compartment fire sources in different facade fire standard tests. Two key factors, the temperature profile of spilled facade plume and the heat flux on the facade surface, are selected to match different large-scale tests.

5.1. Equivalent fire HRR for matching heat flux

In the model, the facade fire scenarios are varied by changing the total fire HRR set inside the chamber. Fig. 9(a) shows the modeled average heat flux on the facade surface within 0.5 m above the opening under different total fire HRR. The average heat fluxes within 0.2 m above the opening are given in Fig. A2 of the Appendix, where the trends of curves are similar.

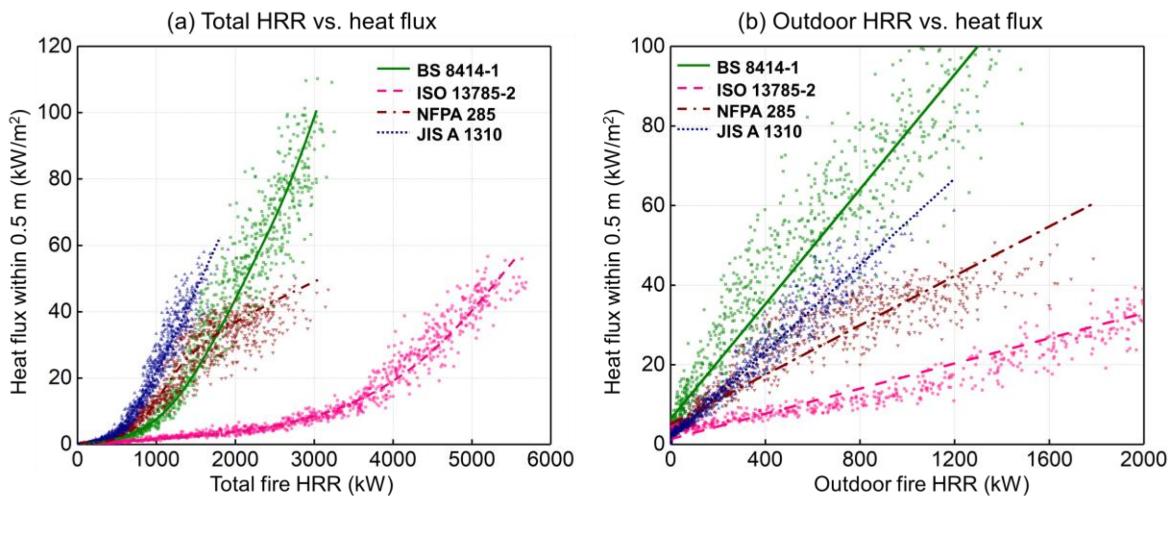

Fig. 9. The relationship of (a) total fire HRR vs. surface heat flux within 0.5 m above the opening and (b) outdoor fire HRR vs. surface heat flux for modeling different large-scale facade fire tests.

Clearly, as the fire HRR increases, the spilled facade flame and fire plume of all tests becomes hotter and stronger, and the heat flux on the facade sample becomes more intensive. Initially, the increase of heat flux in the BS 8414-1 test is slower, compared to JIS A 1310 and NFPA 285, because it has the largest opening and needs the largest HRR to reach the Kawagoe limit or the over-ventilation fire (see Table 1). Note that heat flux is not always related to increasing fire HRRs, as it is also affected by the opening width. Thus, the NFPA 285 cannot reach 50 kW/m^2, regardless of the total HRR, unless the extra external burner is adopted.

Fig. 9(b) plots the relationship between outdoor fire HRR and the heat flux on the facade surface (within 0.5 above the opening). Note that the extra window burner in the NFPA 285 test is removed when increasing the total fire HRR. As expected, the heat flux is more directly related to the outdoor fire HRR, and essentially, a near-linear correlation can be found for all tests with $R^2 > 0.9$ as

- BS 8414-1: $\dot{q}'' = 0.072 \times \mathrm{HRR_{out}} + 6.8$ [kW/m^2]
- NFPA 285: $\dot{q}'' = 0.031 \times \mathrm{HRR_{out}} + 5.0$ [kW/m^2]
- ISO 13785-2: $\dot{q}'' = 0.016 \times \mathrm{HRR_{out}} + 1.3$ [kW/m^2]
- JIS A 1310: $\dot{q}'' = 0.054 \times \mathrm{HRR_{out}} + 1.5$ [kW/m^2]

where the unit of outdoor fire HRR is kW, and the unit of surface heat flux ($\dot{q}''$) is kW/m^2.

In short, it is possible to have the same regional heat flux on the facade sample by adjusting the fire scenario or the value of fire HRR without any setup change in tests. The same heat flux in the specified area can ensure that the samples have an equal probability of ignition in all tests. Table 3 summarizes several typical values of equal heat flux on facade and their equivalent total fire HRRs for different tests. Note that the outdoor HRR is not listed, because its value cannot be directly set or measured in the test. For example, taking the average heat flux of 20 kW/m^2 as the matching value, we can find that the required total fire HRR of JIS A 1310 is 900 ±100 kW (close to the recommended value in the standard). To match the same heat flux of 20 kW/m^2 on the facade sample, the NFPA 285, BS 8414-1, and ISO 13785-2 tests need to set the equivalent total HRR of 1200 ±150 kW, 1400 ±100 kW, and 4000 ±300 kW, respectively.

Table 3. Typical matching parameters and their equivalent fire scenarios (i.e., the total HRR set in chamber) for different large-scale facade fire standard tests.

Matching parameter	Set value	Chamber fire HRR (kW)			
		BS 8414-1 or GB/T 29416	**NFPA-285***	**ISO 13785-2**	**JIS A 1310**
No matching	Default	3,000 kW	1,300 kW	5,600 kW	~900 kW
Average ignition heat flux within 0.5 m above opening	10 kW/m^2	1,100 ±100 kW	900 ±100 kW	3,200 ±200 kW	700 ±50 kW
	20 kW/m^2	1,400 ±100 kW	1,200 ±150 kW	4,000 ±300 kW	950 ±100 kW
	30 kW/m^2	1,600 ±200 kW	1,550 ±250 kW	4,500 ±300 kW	1,150 ±150 kW
	40 kW/m^2	1,800 ±250 kW	2,250 ±300 kW	4,950 ±250 kW	1,300 ±150 kW
	50 kW/m^2	2,100 ±400 kW	3,000 ±200 kW	5,250 ±150 kW	1,500 ±200 kW
Average fire plume temperature within 0.5 m above opening	300 ℃	800 ±100 kW	500 ±80 kW	3,800 ±400 kW	650 ±80 kW
	400 ℃	1,100 ±150 kW	700 ±100 kW	4,250 ±450 kW	800 ±100 kW
	500 ℃	1,400 ±150 kW	1,000 ±200 kW	4,550 ±600 kW	1,000 ±200 kW
	600 ℃	1,750 ±250 kW	1,150 ±250 kW	4,800 ±400 kW	1,150 ±200 kW
Effective ignition height above opening (>500 ℃)	0.1 m	800 kW	700 kW	3,200 kW	500 kW
	0.2 m	1,000 kW	800 kW	3,200 kW	600 kW
	0.5 m	1,250 kW	800 kW	3,950 kW	800 kW

* The fire HRR of the extra window burner outside the chamber is not included.

5.2. Matching the plume temperature and ignition height

The spilled fire plume temperature within 0.5 m above the opening is also matched for different standard tests by changing the total fire HRR, as shown in Fig. 10(a). Similar to the trend of surface heat flux in Fig. 9(a), the temperature also increases with the total fire HRR. Fig. 10(b) plots the relationship between outdoor fire HRR and plume temperature on the facade surface, where a trend of near-linear increase is also observed when the outdoor HRR is above 200 kW, similar to the heat flux curves in Fig. 9(b).

From Fig. 10(a), the equivalent total fire HRRs for different standard tests by matching the spilled fire plume temperature are summarized in Table 3. In other words, by changing fire HRR inside the chamber, the generated spilled fire plume of different tests becomes close to each other. For example, if matching the average plume temperature of 600 ℃ within 0.5 m above the opening, the equivalent fire scenario in the chamber should be set as 1,750 kW (BS 8414-1), 1,150 kW (NFPA 285), 4,800 kW (ISO 13785-2), and 1,150 kW (JIS A 1310), respectively, where the uncertainty is less than 10%.

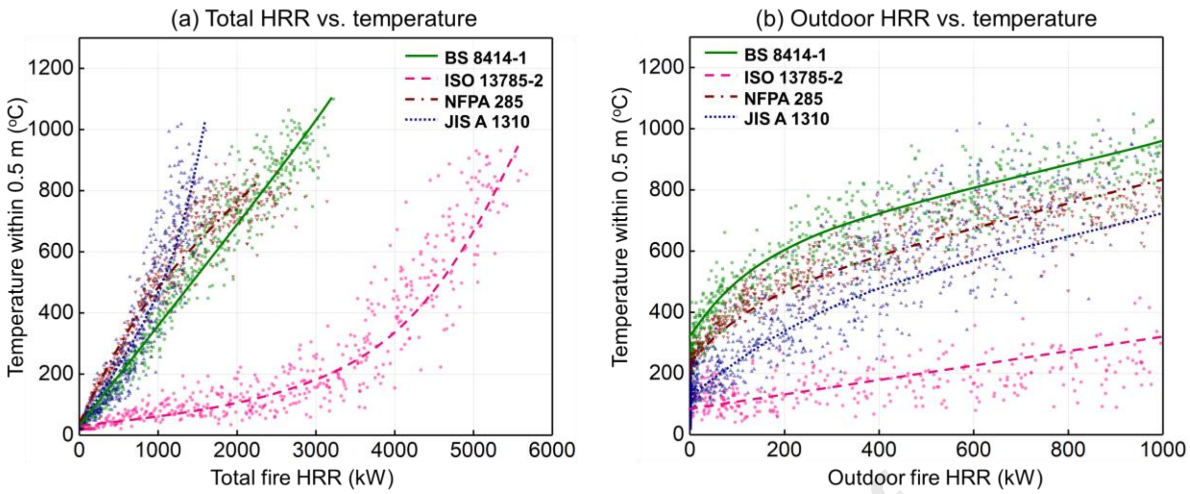

Fig. 10. The relationship of (a) total fire HRR vs. plume temperature within 0.5 m above the opening, and (b) outdoor fire HRR vs. plume temperature for modeling different large-scale facade fire tests.

Table 3 further presents the equivalent fire HRR to get the same effective ignition height above the opening. The threshold plume temperature for ignition is set to 500 ℃. That is, the effective ignition height is the region covered by a hot plume over 500 ℃. Taking an ignition zone of 0.5 m above opening as the match condition, the minimum total fire HRRs can be set as 1,250 kW (BS 8414-1), 800kW (NFPA 285), 3,950 kW (ISO 13785-2), and 800 kW (JIS A 1310), respectively.

In short, by generating the (1) same heat flux on the facade surface, (2) the same average plume temperature, or (3) the same effective ignition height, it is possible to make a relatively fair comparison among different large-scale facade tests. It is difficult to match all these three parameters at the same time, because the dimensions of chamber, opening and facade are different in each test. In practice, the user can decide which matching condition to choose and then adjust the fire HRR inside the chamber accordingly to make a comparison. Of course, these values from numerical simulation call for further verification from the experiments in future work.

6. Conclusions

This study simulates five scenario-based facade fire standard tests, BS 8414-1 (UK), GB/T 29416 (China), ISO 13785-2, NFPA 285 (USA), and JIS A 1310 (Japan). Simulations explore the heat flux and temperature of spilled fire plume that controls the ignition and flame spread of facade fire. Under the default fire scenario, the BS 8414-1 and GB/T 29416 generate the largest heat flux (~100 kW/m^2)

to ignite the facade above the opening. The spilled fire plume in ISO 13785-2 produces a near-constant heat flux (~50 kW/m^2) for 2 m above the opening. The heat flux and plume temperature of NFPA 285 largely depend on the extra window burner, and JIS A 1310 can produce intensive heating on the facade by increasing the chamber fire heat release rate (HRR).

The heat flux and temperature of spilled plume increase almost linearly with the outdoor fire HRR. Thus, by adjusting the total fire HRR, the values of surface heat flux, plume temperature, and ignition height can be matched to enable a fair comparison among different tests. It is a unique investigation to the equivalent scenarios of different facade fire test methods. This work helps understand and compare different facade fire tests that can guide future test development and optimization.

Acknowledgments

This work is funded by the Hong Kong Research Grants Council Theme-based Research Scheme (T22-505/19-N) and the PolyU Emerging Frontier Area (EFA) Scheme of RISUD (P0013879).

References

[1] Aschehoug Ø, Andresen I, Haghighat F, Heiselberg P, Li Y, Olesen BW, et al. State-of-the-art Review: Vol. 1. State-of-the-art Report: NNEX 44: Integrating Environmentally Responsive Elements in Buildings 2008.

[2] Srivastava G, Nakrani D, Ghoroi C. Performance of Combustible Facade Systems with Glass, ACP and Firestops in Full-Scale, Real Fire Experiments. *Fire Technol* 2020;56:1575–98.

[3] Bonner M, Rein G. Flammability and multi-objective performance of building façades: Towards optimum design. *Int J High-Rise Build* 2018;7:363–74.

[4] Čolić A, Pečur IB. Influence of horizontal and vertical barriers on fire development for ventilated façades. *Fire Technol* 2020;56:1725–54.

[5] McLaggan MS, Hidalgo JP, Carrascal J, Heitzmann MT, Osorio AF, Torero JL. Flammability trends for a comprehensive array of cladding materials. *Fire Saf J* 2021;120.

[6] McLaggan MS, Hidalgo JP, Osorio AF, Heitzmann MT, Carrascal J, Lange D, et al. Towards a better understanding of fire performance assessment of façade systems: Current situation and a proposed new assessment framework. *Constr Build Mater* 2021;300:124301.

[7] Schulz J, Kent D, Crimi T, Glockling JLD, Hull TR. A Critical Appraisal of the UK's Regulatory Regime for Combustible Façades. *Fire Technol* 2021;57:261–90.

[8] McKenna ST, Jones N, Peck G, Dickens K, Pawelec W, Oradei S, et al. Fire behaviour of modern façade materials – Understanding the Grenfell Tower fire. *J Hazard Mater*

2019;368:115–23.

[9] Babrauskas V. Facade fire tests: Towards an international test standard. *Fire Technol* 1996;32:219–30.

[10] British Standard BS 8414–1:2020. Fire performance of external cladding systems—Part 1: Test method for non-loadbearing external cladding systems applied to the face of the building. n.d.

[11] Chinese Standards. GB/T 29416-2012 Test method for fire-resistant performance of external wall insulation systems applied to building facades. 2012.

[12] ISO. ISO 13785-2:2002 Reaction-to-fire tests for facades—Part 2: Large-scale test. 2002;2.

[13] Association NFP. NFPA 285 Standard Fire Test method for evaluation of fire propagation characteristics of exterior non-load-bearing wall assemblies containing combustible components. *Natl Fire Prot Assoc Quincy* 2019.

[14] JIS A 1310 Standard Test Test method for fire propagation over building facades 2015.

[15] Khan AA, Lin S, Huang X, Usmani A. Facade Fire Hazards of Bench-Scale Aluminum Composite Panel with Flame-Retardant Core. *Fire Technol* 2021.

[16] Zhou B, Yoshioka H, Noguchi T, Wang K, Huang X. Upward Fire Spread Rate Over Real-Scale EPS ETICS Façades. *Fire Technol* 2021;57:2007–24.

[17] Zhou B, Yoshioka H, Noguchi T, Wang K, Huang X. Fire Technology Fire Performance of EPS ETICS Façade : Effect of Test Scale and Masonry Cover. *Fire Technol* 2022.

[18] Agarwal G, Wang Y, Dorofeev S. Fire performance evaluation of cladding wall assemblies using the 16-ft high parallel panel test method of ANSI/FM 4880. *Fire Mater* 2020.

[19] Jansson R, Anderson J. Experimental and numerical investigation of fire dynamics in a façade test rig. *Proc Fire Comput Model Santander, Spain* 2012;247.

[20] Van Hees P. Development of full-scale façade tests in ISO TC92. MATEC web Conf., vol. 46, EDP Sciences; 2016, p. 1005.

[21] Hostikka S, Bytskov G. Numerical simulations of the ISO 13785-2 façade fire tests. *MATEC Web Conf* 2016;46:1–11.

[22] Anderson J, Boström L, Jansson McNamee R, Milovanović B. Modeling of fire exposure in facade fire testing. *Fire Mater* 2018;42:475–83.

[23] Srivastava G, Gandhi PD. Performance of Combustible Façade Systems Used in Green Building Technologies Under Fire. Springer; 2022.

[24] Sun X, Hu L, Zhang X, Ren F, Yang Y, Fang X. Experimental study on flame pulsation behavior of external venting facade fire ejected from opening of a compartment. *Proc Combust Inst* 2021;38:4485–93.

[25] Ren F, Hu L, Zhang X, Sun X, Zhang J, Delichatsios M. Experimental study of transitional behavior of fully developed under-ventilated compartment fire and associated facade flame height evolution. *Combust Flame* 2019;208:235–45.

[26] Zhang X, Zhang Z, Su G, Tang F, Liu A, Tao H. Experimental study on thermal hazard and

facade flame characterization induced by incontrollable combustion of indoor energy usage. *Energy* 2020;207:118173.

[27] Sun J, Hu L, Zhang Y. A review on research of fire dynamics in high-rise buildings. *Theor Appl Mech Lett* 2013;3:42001.

[28] Anderson J, Boström L, Jansson McNamee R, Milovanović B. Modeling of fire exposure in facade fire testing. *Fire Mater* 2017:475–83.

[29] Anderson J, Boström L, Chiva R, Guillaume E, Colwell S, Hofmann A, et al. European approach to assess the fire performance of façades. *Fire Mater* 2020.

[30] Kernick G. Catastrophe and systemic change: Learning from the Grenfell Tower fire and other disasters. Do Sustainability; 2021.

[31] Wang Y, Bertrand C, Beshir M, Kahanji C, Walls R, Rush D. Developing an experimental database of burning characteristics of combustible informal dwelling materials based on South African informal settlement investigation. *Fire Saf J* 2020;111:102938.

[32] Bonner M, Wegrzynski W, Papis BK, Rein G. KRESNIK: A top-down, statistical approach to understand the fire performance of building facades using standard test data. *Build Environ* 2020;169:106540.

[33] Zhou B, Yoshioka H, Noguchi T, Ando T. Experimental study of expanded polystyrene (EPS) External Thermal Insulation Composite Systems (ETICS) masonery façade reaction-to-fire performance. *Therm Sci Eng Prog* 2018;8:83–92.

[34] Quintiere JG. Principles of fire behavior, Second Edition. 2016.

[35] ISO. ISO 13785-1:2002 Reaction-to-fire tests for facades—Part 2: Intermediate test. vol. 1. 2002.

[36] McGrattan K, Hostikka S, McDermott R, Floyd J, Weinschenk C, Overhold K. Sixth Edition Fire Dynamics Simulator User 's Guide (FDS). *NIST Spec Publ 1019* 2020;Sixth Edit.

[37] McGrattan K, Floyd J, Forney G, Baum H, Hostikka S. Improved radiation and combustion routines for a large eddy simulation fire model. *Fire Saf Sci* 2003:827–38.

[38] McGrattan KB, Baum HR, Rehm RG. Large eddy simulations of smoke movement. *Fire Saf J* 1998;30:161–78.

[39] Zhou B, Yoshioka H, Kanematsu M, Noguchi T. Numerical and experimental study of cedar façade fire. *Fire Mater* 2022;46:476–86.

[40] Cornachini BJ, Foley MW, Knight SS, Ritchey TJ. Calibration of an Intermediate Scale Fire Test Rig for Exterior Wall Assemblies: Source Fire. 2015.

[41] Ren F, Hu L, Sun X, Hu K. An experimental study on vertical temperature profile of facade fire plume ejected from compartment with an opening subjected to external wind normal to facade. *Int J Therm Sci* 2018;130:94–9.

Appendix

Fig. A1 shows the comparison between allowable test values of NFPA 285 and simulation results, including the gas temperature distribution profile and the average heat flux of the facade surface at the centerline above the opening. Results for the first five minutes of the NFPA 285 façade fire test are selected as an example to show the comparison results. Compared with allowable values specified in the standard [13], numerical results of the gas temperature profile at the centerline above the opening is within the average temperatures measured in the experiment. For the gauge heat flux, the simulation results also agree with experimental results and successfully reflect the distribution of heat flux in façade fire tests. The validation results show that the numerical model can better reflect the actual test scenario and can be used to identify equivalent fire scenarios of different test standards.

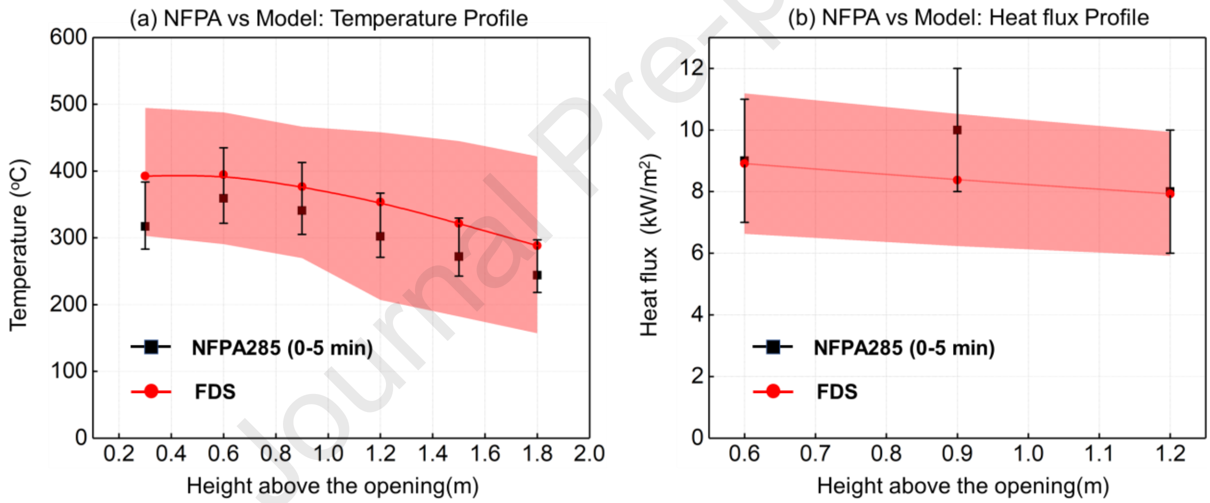

Fig. A1. Validation of NFPA 285 standard tests, experimental vs. numerical data: (a) gas temperature distribution profile, (b) characteristic heat flux of the facade surface at the centerline above the opening, where the shaded area shows the variation in numerical simulations.

Fig. A2 shows the relationship between (a) total fire HRR vs. surface heat flux within 0.2 m above the opening and (b) outdoor fire HRR and surface heat flux for modeling different large-scale facade fire tests. Compared with Fig. 9, we find that the average heat flux values are not sensitive to the size of the ignition area above the opening. For the relationship between outdoor HRR and heat flux in Fig. A2(b), it is also prone to be linear.

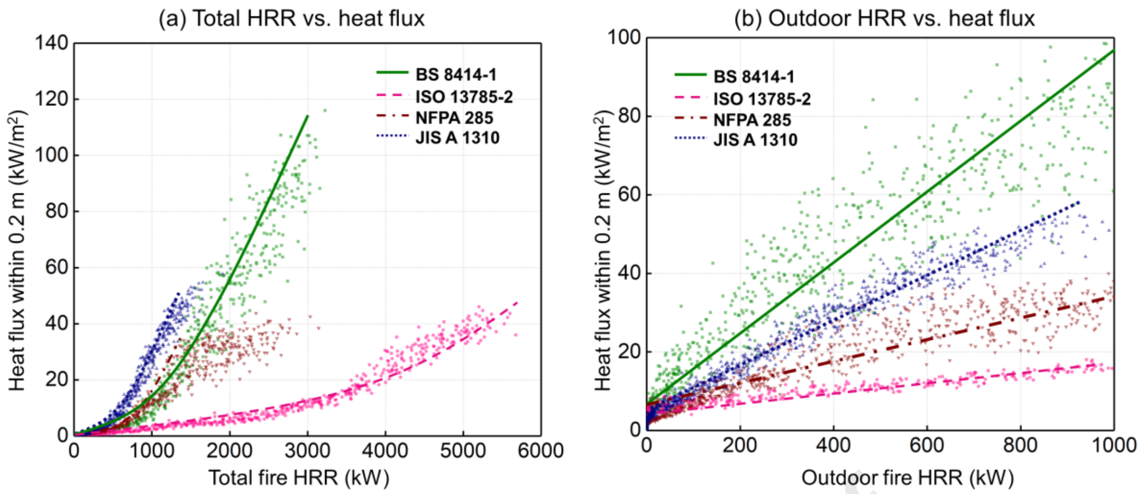

Fig. A2. The relationship of (a) total fire HRR vs. surface heat flux within 0.2 m above the opening, and (b) outdoor fire HRR vs. surface heat flux for modeling different large-scale facade fire tests.

Highlights

- Promote fire safety of facade system to achieve building carbon neutrality.
- Simulate the spilled fire plume for five scenario-based large-scale facade fire tests.
- Reveal the linear correlation between the heat flux on the facade and the outdoor fire HRR.
- Propose the equivalent fire HRRs to enable fair comparison among different standard tests.

CRediT authorship contribution statement

Yizhou Li: Investigation, Writing-original draft, Formal analysis.

Zilong Wang: Investigation, Writing-review & editing, Formal analysis.

Xinyan Huang: Conceptualization, Supervision, Formal analysis, Writing-review & editing, Funding acquisition.

Declaration of interests

☒ The authors declare that they have no known competing financial interests or personal relationships that could have appeared to influence the work reported in this paper.

☐The authors declare the following financial interests/personal relationships which may be considered as potential competing interests: